

LITHIUM PRODUCTION ON A LOW-MASS SECONDARY IN A BLACK HOLE SOFT X-RAY TRANSIENT

SHIN-ICHIRO FUJIMOTO¹, RYUICHI MATSUBA² AND KENZO ARAI³

Submitted to Astrophys. J. Letters

ABSTRACT

We examine production of Li on the surface of a low-mass secondary in a black hole soft X-ray transient (BHSXT) through the spallation of CNO nuclei by neutrons which are ejected from a hot (> 10 MeV) advection-dominated accretion flow (ADAF) around the black hole. Using updated binary parameters, cross sections of neutron-induced spallation reactions, and mass accretion rates in ADAF derived from the spectrum fitting of multi-wavelength observations of quiescent BHSXTs, we obtain the equilibrium abundances of Li by equating the production rate of Li and the mass transfer rate through accretion to the black hole. The resulting abundances are found to be in good agreement with the observed values in seven BHSXTs. We note that the abundances vary in a timescale longer than a few months in our model. Moreover, the isotopic ratio ${}^6\text{Li}/{}^7\text{Li}$ is calculated to be about 0.7–0.8 on the secondaries, which is much higher than the ratio measured in meteorites. Detection of such a high value is favorable to the production of Li via spallation and the existence of a hot accretion flow, rather than an accretion disk corona system in quiescent BHSXT.

Subject headings: Accretion, accretion disks — black hole physics — nuclear reactions, nucleosynthesis, abundances — stars: abundances

1. INTRODUCTION

High abundances of Li have been detected in late-type secondaries of black hole soft X-ray transients (BHSXTs) and a neutron star soft X-ray transient (NSSXT) in quiescence (Martin et al. 1992, 1994, 1996), though Li would be destructed in a deep convective envelope of a late-type star. The Li enrichment has not, however, been observed on a late-type secondary in a compact binary with a white dwarf (Martin et al. 1995). These facts strongly suggest that a production mechanism of Li operates in compact binaries (Yi & Narayan 1997; Guessoum & Kazanas 1999) and that the nature of the primaries is crucial for the mechanism, though rotation might reduce the destruction of Li in the envelope of the secondary (Maccarone et al. 2005).

Multi-wavelength spectra of BHSXTs in quiescence are successfully fitted to the radiation from an advection-dominated accretion flow (ADAF) around the black hole (Narayan et al. 1996, 1997). Density is so low in ADAF, that ions interact inefficiently with electrons. Consequently ions have high temperatures due to viscous heating up to about 30 MeV near the inner edge of ADAF. At such high temperatures, α - α reaction proceeds to synthesize Li inside ADAF (Martin et al. 1994; Yi & Narayan 1997). It is necessary that a fraction $10^{-3} - 10^{-4}$ of the accreting gas is transported to the secondary to explain the high abundances of Li observed in BHSXTs. However, such a high fraction is uncertain to be realized due to strong gravity of the black hole and the Coulomb interactions with nuclei inside ADAF (Guessoum & Kazanas 1999).

Helium breaks via spallation with protons to produce neutrons at the inner region of ADAF. A large fraction of neutrons can be ejected from ADAF, because they do not interact

with nuclei through the Coulomb interactions. Neutrons intercepted by the secondary interact with CNO nuclei through spallation to produce Li on the surface (Guessoum & Kazanas 1999). This scenario is of particular interest, because the Li enrichment is anticipated in secondaries only for BHSXTs and NSSXTs, but for white dwarfs as primaries where ADAF cannot attain enough high temperatures to break helium to nucleons there.

In the present paper, we evaluate the Li abundances on the surface of secondaries in BHSXTs, following the scenario proposed by Guessoum & Kazanas (1999). To this end, we use updated binary parameters, such as the mass M of a black hole, the mass M_* and radius R_* of a secondary, mass accretion rates derived from the spectrum fitting of multi-wavelength observation of BHSXTs in quiescence, and cross sections of neutron-induced spallation reactions. Then, we compare the resulting abundances with the observed values, and show that the agreement is quite well. Moreover, we predict the isotopic ratio ${}^6\text{Li}/{}^7\text{Li}$ on the secondaries in BHSXTs.

2. NEUTRON PRODUCTION IN AN ADVECTION DOMINATED ACCRETION FLOW

Temperature of ions in ADAF is comparable to virial temperature, and is given at radius r by (Narayan & Yi 1994, 1995a,b);

$$T = 3.7 \times 10^{12} \frac{r_{\text{in}}}{r} \text{ K} = 31.9 \frac{r_{\text{in}}}{r} \text{ MeV}. \quad (1)$$

Here r_{in} is the radius at the inner edge of ADAF, and is set to be $3r_g$, where r_g is the Schwarzschild radius of the black hole. The number density is also given by

$$n = 1.7 \times 10^{18} \alpha^{-1} m^{-1} \dot{m} \left(\frac{r}{r_{\text{in}}} \right)^{-3/2} \text{ cm}^{-3}, \quad (2)$$

where α is the viscous parameter, $m = M/M_\odot$, and \dot{m} is the mass accretion rate in units of the Eddington accretion rate $\dot{M}_{\text{Edd}} = 1.4 \times 10^{17} m \text{ g s}^{-1}$.

Once the temperatures, densities and drift timescales are specified, we can follow the abundance evolution in ADAF

¹ Department of Electronic Control, Kumamoto National College of Technology, 2659-2 Suya, Koshi, Kumamoto 861-1102, Japan; fujimoto@ec.knct.ac.jp

² Institute for e-Learning Development, Kumamoto University, Kumamoto 860-8555, Japan

³ Department of Physics, Kumamoto University, Kumamoto 860-8555, Japan

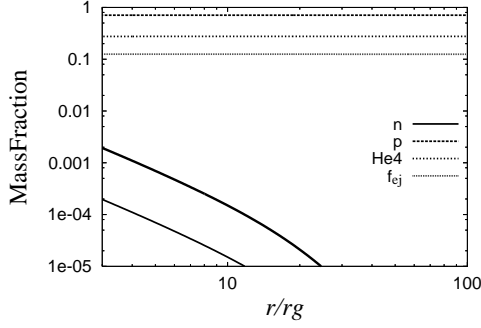


FIG. 1.— Distribution of abundance in ADAF for $\alpha = 0.3$, $m = 10$, and $\dot{m} = 10^{-3}$. The solid, dashed, and dotted lines indicate the mass fractions of n, p, and ${}^4\text{He}$, respectively. The thick solid line denotes the neutron fraction for $\dot{m} = 10^{-2}$. The ejection fraction f_{ej} of neutrons is also presented by the dot-dashed line.

from the outer boundary r_{out} to r_{in} , using a nuclear reaction network. We set r_{out} to be $100r_g$. It is likely that r_{out} becomes much larger during the quiescent state (Narayan et al. 1997), but the abundance of neutrons is independent from the choice of larger r_{out} because of low temperatures (< 1 MeV) in the outer region (Guessoum & Kazanas 1999). Our network contains 17 species of nuclei; n, p, D, T, ${}^3\text{He}$, ${}^4\text{He}$, ${}^9\text{B}$, ${}^{11}\text{C}$, ${}^{12}\text{C}$, ${}^{13}\text{N}$, ${}^{14}\text{N}$, ${}^{15}\text{O}$, ${}^{16}\text{O}$, ${}^{17}\text{F}$, ${}^{20}\text{Ne}$, ${}^{21}\text{Na}$, and ${}^{24}\text{Mg}$, and 14 reactions, whose rates are taken from Table 1 in Guessoum & Gould (1989). It should be emphasized that photodisintegration reactions are not important for abundance evolution inside ADAF, since ADAF is optically thin and photons have no chance to interact with nuclei due to low gas densities (Eq. (2)). Therefore, nuclear statistical equilibrium cannot be realized in ADAF even for high temperatures (Eq. (1)). The network is appropriate for the study of the production of neutrons in ADAF, but insufficient for heavy nuclei as well as Li because of the limited numbers of nuclei and reactions. Initial abundance at r_{out} is set to be the solar composition (Anders & Grevesse 1989).

Figure 1 shows the abundance distribution inside ADAF for $\alpha = 0.3$, $m = 10$, and $\dot{m} = 10^{-3}$. Neutrons are produced significantly via the breakup of ${}^4\text{He}$ at $r < 20r_g$. The distribution of neutrons is similar to that in Figure 1 of Jean & Guessoum (2001). We note that the number fraction of neutrons Y_n depends not on m solely, but on the combination \dot{m}/α^2 . Hereafter we fix $\alpha = 0.3$ in the present paper (Narayan et al. 1997). It should be emphasized that the breakup of helium cannot take place in an accretion corona, which is an alternative scenario to explain multi wavelength spectrum of BHSXTs in quiescence (e.g. Malzac 2007) because of low ion temperatures comparable to electron temperature (< 1 MeV).

The neutrons produced in ADAF have positive Bernoulli numbers (Narayan & Yi 1994), so that a fraction of the neutrons thermally overcomes the deep gravitational well of the black hole before inelastic scattering with protons. The ejection fraction of neutrons f_{ej} is evaluated from Eq. (14) in Guessoum & Kazanas (1990), using the pseudo-Newtonian potential and an experimentally measured cross section of the neutron-proton inelastic scattering, $\sigma_{\text{np}} = 671.0(14.1 \text{ MeV}/E_n) \text{ mb}$ (Tanaka et al. 1970), where E_n is the energy of neutrons. The distribution function of neutrons is set to be Maxwellian with ion temperature of ADAF (Guessoum & Kazanas 1990, 1999). We find that $f_{\text{ej}} \simeq 0.12$, which depends weakly on r as seen from Figure 1. It is noted that f_{ej} is independent of α , m , and \dot{m} .

Using the mass conservation in ADAF, we evaluate the ejection rate of neutrons from ADAF as

$$\begin{aligned} \dot{N}_n &= \int_{r_{\text{in}}}^{r_{\text{out}}} f_{\text{ej}} \left(\frac{dY_n}{dt} \right) \frac{2\pi r \Sigma}{m_n} dr \simeq \frac{\dot{M}}{m_n} Y_{n,\text{in}} f_{\text{ej},\text{in}} \\ &\simeq 1.1 \times 10^{34} \left(\frac{\dot{m}}{10^{-3}} \right) \left(\frac{m}{10} \right) \left(\frac{f_{\text{ej},\text{in}}}{0.1} \right) \left(\frac{Y_{n,\text{in}}}{10^{-4}} \right) \text{ s}^{-1}, \end{aligned} \quad (3)$$

where Σ is the surface density in ADAF, $f_{\text{ej},\text{in}}$ and $Y_{n,\text{in}}$ are the values of f_{ej} and Y_n at r_{in} . Here we have used a relation $df_{\text{ej}}/dr \simeq 0$ (see Figure 1). We note that the rate is unlikely to change significantly for smaller r_{in} . Even if we set $r_{\text{in}} < 3r_g$, the increase in $Y_{n,\text{in}}$ due to higher temperatures would be canceled out by a large decrease in $f_{\text{ej},\text{in}}$ resulted from general relativistic effects.

Next we calculate the energy of the ejected neutrons averaged over the region from r_{in} to r_{out} as

$$\langle E_{\text{ej}} \rangle = \frac{1}{m_n \dot{N}_n} \int_{r_{\text{in}}}^{r_{\text{out}}} E_{\text{ej}} f_{\text{ej}} \left(\frac{dY_n}{dt} \right) 2\pi r \Sigma dr, \quad (4)$$

where E_{ej} is the energy of neutrons ejected from ADAF, and is evaluated from the same way as in f_{ej} . It is noted that $\langle E_{\text{ej}} \rangle$ is crucial for the production of Li on the secondary, because cross sections of both the spallation reactions and the inelastic scattering with protons depend strongly on the neutron energy. We find that $\langle E_{\text{ej}} \rangle \simeq 78 \text{ MeV}$, which is insensitive to α , m , and \dot{m} .

3. LI PRODUCTION ON THE SECONDARY THROUGH SPALLATION OF CNO NUCLEI BY NEUTRONS

The surface of a secondary in BHSXT is bombarded by neutrons from ADAF. We note that β -decays of neutrons can be ignored, because their half-life is much longer than the elapsed time $230(a/R_\odot)(0.1/v_{\text{ej}}) \text{ s}$ during the flight from ADAF to the surface, where a and v_{ej} are the binary separation and the ejection velocity in units of the velocity of light. The depth of an envelope exposed by neutrons is expressed as $1/n_p \sigma_{\text{np}}$, where n_p is the number density of protons on the surface of the secondary, since the neutron-proton inelastic scattering is predominant. The mass of the neutron-exposed envelope is given by

$$M_{\text{exp}} \simeq 2.3 \times 10^{-10} \left(\frac{R_*}{0.7R_\odot} \right)^2 \left(\frac{0.9}{Y_p} \right) \left(\frac{121 \text{ mb}}{\sigma_{\text{np}}} \right) M_\odot. \quad (5)$$

The abundance of Li increases through the spallation of CNO nuclei by neutrons on the surface of the secondary. For isotropic ejection of neutrons from ADAF, the production rate of Li on the secondary is given by

$$\begin{aligned} \dot{M}_{\text{Li}}^+ &= \frac{1}{2} \frac{\dot{N}_n}{4\pi a^2} \sigma_{\text{sp}} M_{\text{exp}} Y_{\text{CNO}} \bar{A}_{\text{Li}} \\ &\simeq 1.6 \times 10^{-20} \left(\frac{\dot{m}}{10^{-3}} \right) \left(\frac{m}{10} \right) \left(\frac{f_{\text{ej},\text{in}}}{0.1} \right) \left(\frac{0.9}{Y_p} \right) \left(\frac{Y_{n,\text{in}}}{10^{-4}} \right) \\ &\quad \times \left(\frac{Y_{\text{CNO}}}{10^{-3}} \right) \left(\frac{\sigma_{\text{sp}}}{25 \text{ mb}} \right) \left(\frac{121 \text{ mb}}{\sigma_{\text{np}}} \right) \left(\frac{R_*}{0.25a} \right)^2 M_\odot \text{ yr}^{-1}, \end{aligned} \quad (6)$$

where \bar{A}_{Li} is the average mass number of Li, which is composed of ${}^6\text{Li}$ and ${}^7\text{Li}$, and is set to be 7, σ_{sp} is the total cross section of the spallation reactions of CNO nuclei, and Y_{CNO} is the number fraction of CNO nuclei, which is 1.2×10^{-3} for the solar abundances (Anders & Grevesse 1989). A factor

1/2 in Eq. (6) means the fact that a half of the surface of the secondary is exposed by neutrons from ADAF.

On the other hand, a fraction of the produced Li is transported to the black hole through accretion. The mass transfer rate of Li from the envelope is expressed as

$$\dot{M}_{\text{Li}}^- \simeq 1.5 \times 10^{-20} \left(\frac{Y_{\text{Li}}}{10^{-10}} \right) \left(\frac{m}{10} \right) \left(\frac{\dot{m}}{10^{-3}} \right) M_{\odot} \text{ yr}^{-1}. \quad (7)$$

It should be noted that the destruction rate of Li in the envelope is $7M_{\text{exp}}Y_{\text{Li}}/t_{\text{des}}$, which is much smaller than \dot{M}_{Li}^- even for a short destruction timescale $t_{\text{des}} \simeq 10^7 \text{ yr}$.

For equilibrium between the production and loss rates \dot{M}_{Li}^+ and \dot{M}_{Li}^- , one can obtain

$$Y_{\text{Li,eq}} \simeq 1.1 \times 10^{-10} \left(\frac{f_{\text{ej,in}}}{0.1} \right) \left(\frac{Y_{\text{n,in}}}{10^{-4}} \right) \left(\frac{0.9}{Y_{\text{p}}} \right) \left(\frac{Y_{\text{CNO}}}{10^{-3}} \right) \times \left(\frac{\sigma_{\text{sp}}}{25 \text{ mb}} \right) \left(\frac{121 \text{ mb}}{\sigma_{\text{np}}} \right) \left(\frac{R_*}{0.25a} \right)^2. \quad (8)$$

It should be emphasized that $Y_{\text{Li,eq}}$ depends on α and \dot{m} as the combination of \dot{m}/α^2 through $Y_{\text{n,in}}$.

The timescale for the Li enhancement is given by

$$\tau_{\text{eq}} = M_{\text{exp}} \bar{A}_{\text{Li}} Y_{\text{Li,eq}} / \dot{M}_{\text{Li}}^+ \simeq 10.2 \left(\frac{f_{\text{ej,in}}}{0.1} \right)^{-1} \left(\frac{Y_{\text{Li,eq}}}{10^{-10}} \right) \left(\frac{Y_{\text{n,in}}}{10^{-4}} \right)^{-1} \left(\frac{Y_{\text{CNO}}}{10^{-3}} \right)^{-1} \times \left(\frac{m}{10} \right)^{-1} \left(\frac{\dot{m}}{10^{-3}} \right)^{-1} \left(\frac{a}{3R_{\odot}} \right)^2 \left(\frac{25 \text{ mb}}{\sigma_{\text{sp}}} \right) \text{ yr}. \quad (9)$$

Therefore, it takes a few years for lithium to achieve the equilibrium abundance of 10^{-10} . We note that the Li abundance varies in a timescale longer than a few months in our model, while this is not the case in the scenario proposed by Yi & Narayan (1997).

Finally, we evaluate the total cross sections of spallation reactions of CNO nuclei induced by neutrons as the sum of the cross sections of ^{12}C , ^{14}N , and ^{16}O weighted by their number fractions. The cross sections for ^{12}C , ^{14}N , and ^{16}O are calculated from the Talys nuclear reaction code (Koning, Hilaire & Duijvestijn 2005). The energy distribution of neutrons just before the spallation is assumed to be the same as that of neutrons ejected from ADAF, because neutrons are unlikely to lose their energies largely during the flight. For the solar abundance and $E_{\text{n}} = \langle E_{\text{ej}} \rangle = 78 \text{ MeV}$, we find that the cross sections are $\sigma_{\text{sp6}} = 10.5 \text{ mb}$ and $\sigma_{\text{sp7}} = 15.3 \text{ mb}$ for the production of ^6Li and ^7Li , respectively, yielding the sum $\sigma_{\text{sp}} = \sigma_{\text{sp6}} + \sigma_{\text{sp7}} = 25.8 \text{ mb}$. If we adopt the abundance of CNO-processed material, in which all the original ^{12}C are converted to ^{14}N through CNO cycle in the interior of the secondary, the total cross section decreases to be $\sigma_{\text{sp}} = 18.0 \text{ mb}$. It is noted that the cross section of the spallation σ_{sp} is smaller than that of the inelastic scattering σ_{np} by a factor 5 at $E_{\text{n}} = 78 \text{ MeV}$.

4. COMPARISON WITH OBSERVATIONS

We compare the evaluated and observed abundances of Li in seven BHSXTs, using updated parameters of the binaries in Table 1. The radii of the secondaries are taken from the simulations of the evolution of (single) spherical stars with corresponding masses and the solar metallicity

TABLE 1
PARAMETERS OF BHSXTs

object	M (M_{\odot})	M_* (R_{\odot})	a (R_{\odot})	P_{orb} (day)	$A(\text{Li})_{\text{obs}}$
XTE J1118+480	6.8	0.25	1.4	0.171	<1.86
GRO 0422+32 ^a	9	0.39	2.3	0.212	<1.62
A0620-003 ^b	9.7	0.65	3.6	0.323	2.31 ± 0.21
QZ Vul	8.5	0.5	2.6	0.345	2.20 ± 0.50
GU Mus	6	0.8	3.3	0.433	3.00 ± 0.50
Nova Oph77	4.9	0.7	2.9	0.521	<2.96
V404 Cyg ^c	12	0.7	3.8	6.47	2.70 ± 0.20

NOTE. — M , M_* , and P_{orb} are taken from Charles & Coe (2006) and Chen et al. (1997). $A(\text{Li})_{\text{obs}} = \log(Y_{\text{Li}}/Y_{\text{p}}) + 12$ is adopted from table 5 in Casares et al. (2007).

^a Bradley et al. (2007)

^b Froning et al. (2007)

^c Esin et al. (1998) and reference therein

at 1Gyr (Table 2 in Chabrier & Baraffe 1997); They vary from $0.21R_{\odot}$ to $0.67R_{\odot}$ as the secondary masses increase. The binary separations are calculated from $R_*/a = 0.46(1 + M/M_*)^{-1/3}$ (Paczynski 1971). The observed abundances of Li are adopted from Casares et al. (2007). We note that an upper limit of $A(\text{Li})_{\text{obs}}$ for GRO 0422+32 was evaluated as a higher value (2.0; Martin et al. 1996), instead of 1.62 (Casares et al. 2007), which has been obtained from the reanalysis of observational data by Martin et al. (1996).

The mass accretion rates in ADAF are found from the spectrum fitting of the multi-wavelength observations of quiescent BHSXTs to be $\dot{m}_{\text{spe}} = 4.3 \times 10^{-3}$ and 2.0×10^{-2} for A0620-003 and V404 Cyg, respectively (Narayan et al. 1997; Quataert & Narayan 1999). For the other objects, where the spectrum fitting has not yet been performed in quiescence, we simply specify the accretion rates from the minimum X-ray luminosities in these systems (Garcia et al. 2001; McClintock et al. 2003). These values of \dot{m}_{spe} are given in Table 2.

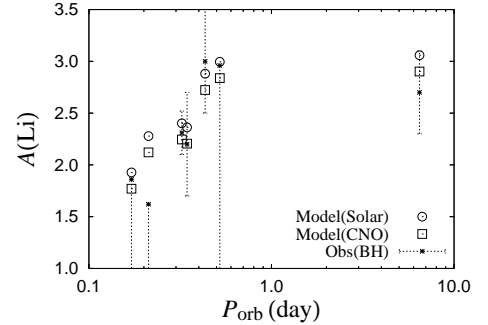


FIG. 2.— Evaluated and observed abundances of Li on the secondaries in seven BHSXTs with respect to their orbital periods.

Using these values of parameters all together, we calculate the equilibrium abundances of Li on the secondaries in seven BHSXTs. The resulting abundances $A(\text{Li}) = \log(Y_{\text{Li,eq}}/Y_{\text{p}}) + 12$ and the enhancement timescale τ_{eq} are given in Table 2. We show $A(\text{Li})$ against the orbital periods P_{orb} of the binaries by the open circles in Figure 2. It is found that our results are in good agreement with the observed abundances, in particular for $P_{\text{orb}} \geq 0.3 \text{ day}$.

If we adopt the composition of CNO-processed material for the secondary, we obtain lower abundances of Li, as denoted

TABLE 2
ABUNDANCES OF LI AND ACCRETION RATES.

object	$A(\text{Li})$	\dot{m}_{spe}	\dot{m}_{bf}	$\dot{m}_T/3$	τ_{eq} (yr)
XTE J1118+480	1.93	2.0e-3	1.7e-3	1.3e-3	0.63
GRO 0422+32	2.28	4.0e-3	8.8e-4	1.8e-3	0.44
A0620-003	2.40	4.3e-3	3.2e-3	2.4e-3	2.06
QZ Vul	2.36	4.0e-3	2.7e-3	1.6e-3	0.94
GU Mus	2.88	8.0e-3	1.1e-2	4.3e-3	3.40
Nova Oph77	3.00	1.0e-2	9.2e-3	4.5e-3	1.86
V404 Cyg	3.06	2.0e-2	8.7e-3	1.7e-2	0.18

by the open squares in Figure 2. This is favorable to BHSXTs with $P_{\text{orb}} < 0.3$ day, such as XTE J1118+480 (Ergma & Sarna 2001; Haswell et al. 2002).

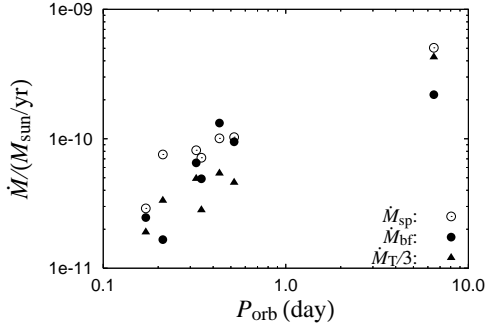


FIG. 3.— Mass accretion rates with respect to the orbital periods.

Next, we try to fit our results to the observed Li abundances with varying accretion rates. The resulting best-fit rates \dot{m}_{bf} are given in Table 2. It is found that they are comparable to or slightly lower than \dot{m}_{spe} . They are also nearly 1/3 of the rates \dot{m}_T predicted by binary evolution models (King et al. 1996), where a factor 1/3 is taken into account with the accumulation of accreting material in an outer thin disk (Menou et al. 1999). Figure 3 shows the comparison of the mass accretion rates \dot{M}_{spe} , \dot{M}_{bf} , and $\dot{M}_T/3$ with respect to the orbital periods in BHSXTs.

Finally, we evaluate the isotopic ratio ${}^6\text{Li}/{}^7\text{Li}$ on the secondaries. It is easily calculated from the cross sections

of ${}^6\text{Li}$ and ${}^7\text{Li}$ for the spallation reactions to be 0.69 – 0.81, depending on the CNO abundances of the secondaries. We note that the ratio is much larger than 0.12 for NSSXT Cen X-4 (Casares et al. 2007) and 0.081 for meteorites (Anders & Grevesse 1989). Detection of such a high ${}^6\text{Li}/{}^7\text{Li}$ ratio will be an evidence for the production of Li on the secondaries in BHSXTs.

5. SUMMARY

We have evaluated the Li abundances on the surface of the low-mass secondaries in quiescent BHSXTs, using the updated parameters of the binaries and the cross sections of neutron-induced spallation reactions. The mass accretion rates in ADAFs are derived from the spectrum fitting of multi-wavelength observations (Narayan et al. 1997; Quataert & Narayan 1999) or specified from the minimum X-ray luminosities of BHSXTs. Significant amounts of Li are produced on the surface through the spallation of CNO nuclei by neutrons which are ejected from hot ADAFs around the black hole. We have obtained the equilibrium abundances of Li by equating the production rate of Li on the secondary and the mass transfer rate through accretion to the black hole. It is found that the resulting abundances are in good agreement with the observed values in seven BHSXTs. We emphasize that the abundances vary in a timescale longer than a few months in our model. Note also that the isotopic ratio ${}^6\text{Li}/{}^7\text{Li}$ becomes 0.69–0.81 on the secondaries in BHSXTs. Detection of such a high ratio will be favorable to the production of Li through the spallation on the secondaries and to the existence of ADAF, rather than an accretion disk corona system (e.g. Malzac 2007).

Although we have concentrated ourselves on the case of BHSXTs in the present paper, the scenario for the production of Li is also applicable to the secondaries of NSSXTs, such as Cen X-4, with a modification on the geometry of ADAF due to the magnetic fields of a neutron star.

We can evaluate abundances of Be and B produced via the neutron-induced spallation and γ -ray lines emitted through neutron capture on a secondary. This is our future task.

REFERENCES

- Anders, E., & Grevesse, N. 1989, *Geochim. Cosmochim. Acta* 53, 197
Bradley, C. K., Hynes, R. I., Kong, A. K. H., Haswell, C. A., Casares, J., & Gallo, E. 2007, *astro-ph* 0706.2652
Casares, J., Bonifacio, P., González Hernández, J. I., Molaro, P., & Zoccali, M. 2007, *A&A*, 470, 1033
Chabrier, G., & Baraffe, I. 1997, *A&A*, 327, 1039
Chares, P. A., & Coe, M. K. 2006 in *Compact Stellar X-ray Sources*, eds. W.H.G. Lewin, M. van der Klis, Cambridge Univ. Press
Chen, W., Shrader, C. R., & Livio, M. 1997, *ApJ*, 491, 312
Ergma, E., & Sarna, M. J. 2001, *A&A*, 374, 195
Esin, A. A., Narayan, R., Cui, W., Grove, J. E., & Zhang, S.-N. 1998, *ApJ*, 505, 854
Froning, C. S., E. L., & Bitner, M. A. 2007, *ApJ*, 663, 1215
Garcia, M. R., McClintock, J. E., Narayan, R., Callanan, P., Barret, D., & Murray, S. S. 2001, *ApJ*, 553, L47
Guessoum, N., & Gould, R. J. 1989, *ApJ*, 345, 356
Guessoum, N., & Kazanas, D. 1990, *ApJ*, 358, 525
Guessoum, N., & Kazanas, D. 1999, *ApJ*, 512, 332
Haswell, C. A., Hynes, R. I., King, A. R., & Schenker, K. 2002, *MNRAS*, 332, 928
Jean, P., & Guessoum, N. 2001, *A&A*, 378, 509
King, A. R., Frank, J., Kolb, U., & Ritter, H. 1996, *ApJ*, 467, 761
Koning, A. J., Hilaire, S., & Duijvestijn, M. C. 2005, *Proc. Int. Conf. on Nuclear Data for Science and Technology*, ed. C. Haight et al., AIP Conf., 769, 1145
Maccarone, T. J., Jonker, P. G., & Sills, A. I. 2005, *A&A*, 436, 671
Malzac, J. 2007, *Memorie della Societa Astronomica Italiana*, 78, 382
Martin, E. L., Rebolo, R., Casares, J., & Charles, P. A. 1992, *Nature*, 358, 129
Martin, E. L., Rebolo, R., Casares, J., & Charles, P. A. 1994, *ApJ*, 435, 791
Martin, E. L., Casares, J., Charles, P. A., & Rebolo, R. 1995, *A&A*, 303, 785
Martin, E. L., Casares, J., Molaro, P., Rebolo, R., & Charles, P. 1996, *New Astron.* 1, 197
McClintock, J. E., Narayan, R., Garcia, M. R., Orosz, J. A., Remillard, R. A., & Murray, S. S. 2003, *ApJ*, 593, 435
Menou, K., Esin, A. A., Narayan, R., Garcia, M. R., Lasota, J.-P., & McClintock, J. E. 1999, *ApJ*, 520, 276
Narayan, R., & Yi, I. 1994, *ApJ*, 428, L13
Narayan, R., & Yi, I. 1995a, *ApJ*, 444, 231
Narayan, R., & Yi, I. 1995b, *ApJ*, 452, 710
Narayan, R., McClintock, J. E., & Yi, I. 1996, *ApJ*, 457, 821
Narayan, R., Barret, D., & McClintock, J. E. 1997, *ApJ*, 482, 448
Paczynski, B. 1971, *ARA&A*, 9, 183
Quataert, E., & Narayan, R. 1999, *ApJ*, 520, 298

Tanaka, M., Koori, N., & Shirato, S. 1970, J. Phys. Soc. Jpn, 28, 11
Yi, I., & Narayan, R. 1997, ApJ, 486, 363